A red tide alga grown under ocean acidification up-regulates its tolerance to lower pH by increasing its photophysiological functions

Running Title: *Phaeocystis globosa* and ocean acidification

Shanwen Chen[1,2], John Beardall[3] and Kunshan Gao[2]*

[1] Marine Biology Institute, Shantou University, Shantou 515063, China

[2] State Key Laboratory of Marine Environmental Science, Xiamen University, Xiamen, 361005, China

[3] School of Biological Sciences, Monash University, Clayton, VIC 3800, Australia

[*] Author for correspondence: Email, ksgao@xmu.edu.cn; Tel, 86-592-2187982; Fax, 86-592-2187963

Key words: CO_2, acidification, light, PAR, *Phaeocystis globosa*

Abstract:

Phaeocystis globosa, a red tide alga, often forms blooms in or adjacent to coastal waters and experiences changes of pH and seawater carbonate chemistry caused by either diel/periodic fluctuation in biological activity, human activity or, in the longer term, ocean acidification due to atmospheric CO_2 rise. We examined the photosynthetic physiology of this species while growing it under different pH levels induced by CO_2 enrichment and investigated its acclimation to carbonate chemistry changes under different light levels. Short-term exposure to reduced pH_{nbs} (7.70) decreased the alga's photosynthesis and light use efficiency. However, acclimation to the reduced pH level for 1-19 generations led to recovered photosynthetic activity, being equivalent to that of cells grown under pH 8.07 (control), though such acclimation required a different time span (number of generations) under different light regimes. The low-pH grown cells increased their contents of chlorophyll and carotenoids with prolonged acclimation to the acidification, with increased photosynthetic quantum yield and decreased non-photochemical quenching. The specific growth rate of the low-pH grown cells also increased to emulate that grown under the ambient pH level. This study clearly shows that *Phaeocystis globosa* is able to acclimate to seawater acidification by increasing its energy capture and decreasing its non-photochemcial energy loss.

1 Introduction

Ocean acidification (OA) is another global environmental problem caused by increasing atmospheric CO_2, which is projected to increase up to 1000 ppmv by 2100, based on the IPCC A1F1 scenario (business as usual scenario) (IPCC, 2007). Increasing pCO_2 in seawater causes a decrease in pH (ocean acidification, OA) and brings about chemical changes in the seawater carbonate chemistry, decreasing carbonate ion concentration and increasing bicarbonate ions. On the other hand, in coastal waters, interactions of OA with eutrophication and deoxygenation are suggested to induce faster pH declines compared to pelagic waters (Cai et al., 2011), though day-night pH fluctuations are large due to high productivity and respiration (Cornwall et al., 2013).

Effects of the CO_2 enrichment on phytoplankton have been widely studied (see the reviews, and literature therein, by Beardall et al., 2009; Tanaka et al., 2013; Brussaard et al., 2013; Gao and Campbell, 2014). Algal responses to elevated CO_2 concentrations have indicated a stimulation of growth or photosynthesis (Gao et al., 1991; Hein and Sand-Jensen, 1997; Zou et al., 2011; Trimbon et al., 2013), reduced calcification (Riebesell et al., 2000; Gao and Zheng, 2010) or growth rates (Gao et al., 2012b; Trimbon et al., 2013) or stimulation of respiration (Wu et al., 2010; Yang and Gao, 2012). Other reports have indicated neutral responses with insignificant influences on growth (Arnold et al., 2013), calcification (Langer et al., 2006, 2009) or photosynthesis (Wu et al., 2008; Trimbon et al., 2013). While elevated CO_2 in air, and hence in water, might stimulate algal photosynthesis, the CO_2-induced pH-drop and change in carbonate chemistry of seawater could bring about different physiological impacts on phytoplankton (Raven, 2011; Gao and Campbell, 2014). It is known for instance that OA stimulates non-photochemical quenching when diatoms or surface phytoplankton assemblages are grown under bright sunlight (Gao et al., 2012b). Neverthless, the balance between CO_2 enrichment and negative impacts of lower pH could act to minimize

the observable effects of OA, so that, overall, neutral reponses would be recorded. Recently, it has been shown that the effects of OA on diatoms could be stimulatory, neutral or inhibitory for growth depending on the levels of solar radiation or depth in the water column (Gao et al., 2012b).

Phaeocystis globosa, a heteromorphic marine phytoplankter, forms gelatinous colonies during blooms (Schoemann et al., 2005; Peperzak and Poelman, 2008) but predominantly lives as flagellated solitary cells (Rousseau et al., 2007; Peperzak and Gäbler-Schwarz, 2012). This organism is known to operate highly efficient CO_2 concentrating mechanisms (Rost et al., 2003; Chen and Gao, 2011), tolerate high solar UV irradiances (Chen and Gao, 2011), acclimate flexibly to the changes in PAR light intensity (Schoemann et al., 2005) and show strain-specific responses to elevated CO_2 (Wang et al., 2010; Hoogstraten et al., 2012). In the present study, we exposed cells of *Phaeocystis globosa* to a range of light and pH levels, and found that this species can readily acclimate to changes in seawater carbonate chemistry caused by OA, with different rates of acclimation under different light levels.

2 Materials and methods

2.1 Organism and culture conditions

Phaeocystis globosa Scherffel (ST-97) was isolated from a bloom in the Southern China Sea in 1997 (Chen et al., 2002) and has been maintained thereafter at Xiamen University as an axenic unialgal culture growing in modified f/2 medium (Si not enriched). We chose the flagellated form for this study since this accounts for most of the time during the life cycle of *P. globosa* and is responsible for the occurrence of Harmful Algal Blooms (HAB) (Rousseau et al., 2007; Peperzak and Gäbler-Schwarz, 2012). The flagellated cells (3-8 μm) were grown for 3 days (about 9 generations) in modified turbidostat cultures (Chen and Gao, 2011) under photosynthetically active radiation (PAR) levels of 25, 200, or 800 μmol photons m^{-2} s^{-1} at 20

^{o}C before the cells were used in the following experiments.

2.2 Seawater acidity and its adjustment

We set two ocean acidity treatments of pH_{nbs} 8.07 and 7.70, which represent the mean pH in seawater at the present time and that expected by 2100, respectively, and which are consistent with the recommendations by Barry et al. (2010) for ocean acidification research.

Since photosynthetic carbon fixation often exceeds dissolution (hydration) of CO_2 from aeration in algal cultures, making the pH rise even under elevated CO_2 levels (Gao et al. 1991), the best way to maintain constant pH level is to use continuous cultures while maintaining low cell concentrations (LaRoche et al., 2010). We therefore operated turbidostat cultures in a CO_2 chamber (Conviron EF7, Controlled Environments Limited, Canada), in which designated CO_2 concentrations were automatically achieved by mixing pure CO_2 and ambient air (390 ppmv CO_2), and the cell concentration was maintained within a range of 0.9–1.1×10^5 cells mL^{-1} (Concentrations of Chl a were 0.23–0.64 pg $cell^{-1}$). The medium flow rates (efflux from and influx to the culture) were adjusted in order to maintain stable levels of cell concentration and carbonate chemistry. The turbidostat culture system consisted of a culture vessel (a quartz tube of 1200 mL, 7.0 cm in diameter and 40 cm in length) and a medical transfusion unit for transferring the medium and adjusting the flow rate (Chen and Gao, 2011). The culture vessels were aerated with filtered (SLLG013SL, Millipore, USA, 0.2-μm-pore size) air of 1000 ppmv CO_2 or of ambient CO_2 level to adjust the pH in the cultures to 7.70 or 8.07. The aeration rate was adjusted within a range of 700–900 $mL \cdot min^{-1}$ in order to maintain the stability of the seawater carbonate chemistry (change of carbonate system parameters < 3%, Table 1). The pH in the cultures was measured with a pH meter (Seveneasy, Mettler-Toledo, Switzerland), which was frequently calibrated with standard N.B.S. buffer solution (Merck, Germany). The quartz culture tubes were maintained in a water bath for temperature control at 20 ± 1 ^{o}C using a refrigerating circulator (CAP-3000,

Tokyo Rikakikai, Japan).

2.3 Determinations of growth rate and photosynthetic pigments

Since the cultures were operated continuously, the specific growth rate (μ) was calculated as: $\mu = F/V$, where F represents the flow rate and V is the volume of the culture.

Photosynthetic pigments were determined by filtering 100 mL culture through a Whatman GF/F filter, extracting in 5 mL absolute methanol overnight and centrifuging for 10 min (2000 g) at 4 ^{o}C, and measuring the absorbance of the supernatant with a spectrophotometer (DU_{530} DNA/Protein Analyzer, Beckmen Coulter, USA) as previously reported (Gao et al., 2007). Chl *a*, Chl *c* and carotenoids were calculated according to Jeffrey and Welschmeyer (1997) and Ritchie (2006).

2.4 Assessment of photochemical activity

Chlorophyll fluorescence parameters indicative of photochemical activity were determined with a pulse amplitude modulated fluorometer (WATER-ED-PAM, Walz, Germany). The effective quantum yield ($\Phi_{PSII}=\Delta F/F_m'$) was determined on the basis of the instant maximal fluorescence (F_m') and the steady-state fluorescence (F_t) of the light-adapted cells according to Genty et al. (1989): $\Phi_{PSII} =\Delta F/F_m' = (F_m' - F_t) / F_m'$. Nonphotochemical quenching (NPQ) was determined on the basis of the maximal fluorescence (F_m) of the dark-adapted cells at 06:00 h (before the growth light was switched on) and the instant maximal fluorescence (F_m') of the light-adapted cells during daytime as follows: $NPQ= (F_m - F_m') / F_m$ (Bilger and Björkman, 1990). In the course of measuring F_m, F_m' and F_t, the saturating pulse (0.8 s) and actinic light were set at 4000 and 150 μmol photons$\cdot m^{-2}\cdot s^{-1}$, respectively. Rapid light curves (RLCs) were obtained by exposing samples to 10 s of blue light at eight incremental steps of PAR ranging from 0 to 2000 μmol photons m^{-2} s^{-1}. Relative electron transport rate (rETR) was determined according to the following formula: $rETR = \Phi_{PSII}\times I\times F\times 0.5$, where Φ_{PSII} is the photochemical yield in the light, I is the actinic irradiance in μmol quanta m^{-2} s^{-1}, F is the species-specific

fraction of incident quanta absorbed by the cells, and 0.5 is a factor allowing for the fraction of the absorbed light utilized by PSII. Parameters, such as α (photosynthetic light harvesting efficiency; the initial slope of the curve), I_k (irradiance of maximum photosynthesis) and $rETR_{max}$ (maximum rETR), were obtained by fitting a curve to the RLC data in Sigmaplot 2001 (version 7.0, SPSS) according to Platt et al. (1980) and Ralph (2005) using the equation $P = P_m [1 – e^{-(\alpha \times I/Pm)}]$, where P_m is the light-saturated photosynthetic electron transport rate, α the initial slope of the RLC before the onset of saturation, I the photosynthetically active radiation (400–700 nm). The three major constituents of non-photochemical quenching (qN) (Energy-dependent quenching, qE; state transition quenching, qT and photoinhibitory quenching, qI) were determined by dark relaxation measurements after the actinic light had been turned off (Lichtenthaler et al., 2005). For this purpose, a saturating pulse was applied at 1, 5 and 18 min after turning off the actinic light (with the measuring light remaining switched on throughout the dark relaxation measurement of qN), and $F_m'1$, $F_m'5$, and $F_m'18$ were obtained. The corresponding F_V ($F_V = F_m - F_0$) values of the samples were determined before measuring $F_m'1$, $F_m'5$, and $F_m'18$. qE, qT and qI were calculated respectively as follows:

$$qE = (F_m'5 - F_m'1)/F_v \quad (1)$$

$$qT = (F_m'18 - F_m'5)/F_v \quad (2)$$

$$qI = (F_m - F_m'18)/F_v \quad (3)$$

In the above formulae, $F_m'1$, $F_m'5$, and $F_m'18$ represent the maximal Chl fluorescence at 1, 5 and 18 min of the dark relaxation period after turning off the actinic light.

2.5 Determination of photosynthesis and respiration

Photosynthetic oxygen evolution and dark respiration were measured with a Clark-type O_2 electrode (YSI 5300; Yellow Springs Instrument Co., Inc., USA). The cells grown under the low or high CO_2 levels for 1-9 generations were incubated and their

photosynthesis/respiration was measured in the seawater equilibrated with different levels of CO_2 under PAR of 400 μmol photons m^{-2} s^{-1} or in complete darkness, respectively.

2.6 Measurements of dissolved inorganic carbon and total alkalinity

Dissolved inorganic carbon (DIC) was determined using a total carbon analyzer (TOC-5000, Shimadzu, Japan), which automatically measured DIC and TC in the culture supernatant (after centrifugation). Other parameters for the seawater carbonate system were estimated according to the measured values of DIC and pH using the software CO_2SYS (Lewis and Wallace, 1998).

2.7 Data analysis

Paired t-test or One-way ANOVA (Rosner, 2011) was used to establish the significance of differences among the treatments at $p<0.05$.

3 Results

3.1 DIC, pH, CO_{2aq} and TA

When the pH was adjusted from 8.07 to 7.70 by adding CO_2-saturated seawater or aerating with CO_2-enriched air, DIC, CO_{2aq}, and HCO_3^- increased by 11.9%, 164.5% and 12.3%, respectively, and CO_3^{2-} decreased by 51.4% ($p < 0.05$), while TA showed no significant difference between low- and high-CO_2 cultures ($p > 0.05$). All parameters showed no significant changes under the different irradiance levels (LL, low light; ML, middle light; HL, high light) ($p > 0.1$) (Table 1).

3.2 Growth

The effects of acidification on *P. globosa* growth rates were different under 25 (low light: LL), 200 (middle light: ML), and 800 μmol photons m^{-2} s^{-1} (high light: HL).

In the pH8.07 (high pH, HpH) culture, with bubbling using ambient air, the specific growth rates (μ) of the alga under LL, ML and HL were 0.732–0.751, 1.096–1.131 and 1.244–1.269

201 d^{-1}, respectively. Correspondingly, growth rates were 0.732–0.781, 1.054–1.148 and
202 1.013–1.225 d^{-1} in the pH7.70 (low pH, LpH) culture, with bubbling CO_2-enriched air. Under
203 the corresponding light regimes (LL, ML, HL), at day 1 (generation 1), rates were lower by
204 1.4% ($p > 0.05$), 5.3% ($p < 0.05$) and 19.1% ($p < 0.05$), respectively, in the LpH cultures,
205 whereas at day 7 (generation 19) they were higher by 9.1% ($p < 0.05$), 4.6% ($p < 0.05$) and
206 -2.4% ($p > 0.05$), respectively, compared to the HpH cultures (Fig. 1).

207 **3.3 Photosynthetic pigments**

208 Under different irradiances, acidification affected chlorophyll (Chl) and carotenoids (Carot) to
209 different extents. In the HpH culture, bubbled with ambient air, the Chl contents of the cells
210 grown under LL, ML and HL treatments were 0.715–0.759, 0.337–0.344 and 0.223–0.236 pg
211 $cell^{-1}$, respectively; and the Carot levels, 0.290–0.299, 0.318–0.323 and 0.359–0.372 pg $cell^{-1}$.
212 However, in the LpH culture aerated with the CO_2-enriched air, the Chl values were higher by
213 7.7% ($p < 0.05$), 9.7% ($p < 0.05$) and 12.9% ($p < 0.05$), in the LL, ML and HL treatments,
214 respectively, when the cells had acclimated to the acidification by day 7, compared to values
215 at day 1; The corresponding Carot values increased by 19.8% ($p < 0.05$), 12.1% ($p < 0.05$)
216 and 8.8% ($p < 0.05$) (Fig. 2).

217 **3.4 Photosynthetic characteristics**

218 During the continuous cultures under LL, ML and HL, the effective photochemical
219 efficiencies ($\Phi_{PSII} = \Delta F/F_m'$) of the algal cells in the HpH culture ranged from 0.685–0.689,
220 0.569–0.573 and 0.415–0.421, respectively, while the non-photochemical quenching (NPQ)
221 values were 0.367–0.379, 0.569–0.596 and 1.233–1.248 (Fig. 3). On day 1, Φ_{PSII} values were
222 lower by 6.8% ($p < 0.05$), 14.8% ($p < 0.05$) and 39.9% ($p < 0.01$), while NPQ values were
223 higher by 8.4% ($p < 0.05$), 11.5% ($p < 0.05$) and 17.8% ($p < 0.05$), respectively, under the 3
224 light levels in the LpH cultures, compared to those grown in the HpH cultures. At day 7,
225 acclimation to the acidification led to increased Φ_{PSII} values by 11.9% ($p < 0.05$) and 11.3%

($p < 0.05$) under the LL and ML levels, but to a decreased value by -2.3% ($p > 0.05$) under the HL, respectively, in the LpH cultures, compared to that of HpH, while NPQ was also correspondingly higher by 6.8% ($p > 0.05$), 4.6% ($p > 0.05$) and 2.6% ($p > 0.05$) (Fig. 3).

The effects of the seawater acidification on the three major non-photochemical quenching parameters of the alga were similar (Table 2). At day 1 (generation 1) under LL, ML and HL, the acidification increased the energy-dependent quenching (qE) by 28.6% ($p < 0.05$) under LL, 33.3% ($p < 0.05$) under ML and 40.0% ($p < 0.01$) under HL, respectively; the state transition quenching (qT) increased by 36.4% ($p < 0.05$), 26.1% ($p < 0.05$) and 20.0% ($p < 0.05$), and the photoinhibitory quenching (qI) increased by 75.0% ($p < 0.05$), 93.8% ($p < 0.01$) and 121.8% ($p < 0.05$), respectively. By day 7 (about generation 19), when the alga had acclimated to the acidification, qE values were higher by 77.8% ($p <0 .01$), 31.3% ($p < 0.05$) and 14.3% ($p < 0.05$) under LL, ML and HL, respectively, compared to those on day 1; qT values were higher by 13.3% ($p < 0.05$), 18.8% ($p < 0.05$) and 27.8% ($p < 0.05$); and qI values were lower by 14.3% ($p < 0.05$), 41.9% ($p < 0.01$) and 52.9% ($p < 0.01$) (Table 2).

The responses of the alga to identifical CO_2 enrichment (LpH) conditions were different among the different light levels (Fig. 4). At either LL or ML, algal photosynthetic rate initially increased with increasing CO_{2aq} concentration. However, it decreased with further increases in CO_{2aq} concentrations above 26.3 μM or 33.3 μM for the cells grown in the low or the high CO_2, respectively, for 3 days (9 generations) (Fig. 4), with the LpH-grown cells tolerating higher levels of CO_2 (lower levels of pH).

At generation 1 after the CO_2-induced acidification, the algal photosynthetic light harvesting efficiency (α) and maximal photosynthesis rate (P_m) of *P. globosa* decreased from 0.007 mol electrons/mol photons and 0.360 μmol O_2 (μg chl *a*)$^{-1}$ h^{-1} in the HpH culture to 0.003 mol electrons/mol photons and 0.318 μmol O_2 (μg chl *a*)$^{-1}$ h^{-1} in the LpH culture, respectively, representing decreases of 57.1% ($p < 0.01$) and 11.7% ($p < 0.05$), while the light

saturation point (I_k) increased from 51.4 to 106.0 μmol photons m^{-2} s^{-1}, an increase of 106.2% ($p < 0.01$) (Table 3). After 7d (about 19 generations) growth in LpH cultures, the α and P_m values were lowered by 14.3% ($p > 0.05$) and by 1.7% ($p > 0.5$), compared to those in the HpH culture, while the I_k was higher by 14.8% ($p > 0.05$) (Table 3), reflecting an insignificant impact of the acidification after the acclimation.

4. Discussion

The results of this study showed that effects of CO_2-induced acidification on *Phaeocystis globosa* are strongly related to the intensity of irradiance and stage of acclimation to the acidification. Additonally, the present study provides the first evidence that *P. globosa* can adjust to the changes in carbonate chemistry by upregulating its photosynthetic pigments and photoprotective capability with downregulated photoinhibitory non-photochemical quenching, leading to the acclimated cells showing a higher tipping point of CO_{2aq} (lower pH) where net photosynthesis leveled off.

Exposure of the *P. globosa* cells to 1000 ppmv-CO_2-induced acidification reduced its growth rate under the light levels above 200 μmol photons m^{-2} s^{-1}, but led to little effect under low light (LL, 25μmol photons m^{-2} s^{-1}) (Fig. 1). This result is consistent with that reported from Hoogstraten *et al*. (2012), but contradictory to observations, on cells grown under high light, of Wang et al. (2010). However, after the algae had acclimated to the acidification for 3 (9 generations) and 5 (14 generations) days under LL and ML respectively, the enhancement of the growth rate under the high CO_{2aq} (LpH) level became obvious (Fig. 1), which contradicts the findings of Wang et al. (2010) and Hoogstraten et al. (2012), who showed that the growth rate under low light was not influenced by elevated CO_2. Although these findings appear partly inconsistent, even contradictory, they might reflect the fact that the responses of an alga to elevated CO_2 are complex and involve interactions with other environmental

276 factors, such as nutrient levels. In the present study, continuous cultures were operated with a
277 stable supply of nutrients.
278 The photochemical performance of the alga differs between cells grown under different
279 levels of light and pH, with the highest effective quantum yield under LL and LpH, and the
280 highest NPQ under the HL and LpH (Fig. 3). In theory, elevated CO_{2aq} can result in energy
281 savings associated with down-regulation of the energy necessary to operate CO_2 concentrating
282 mechanisms (CCM), thereby improving algal performance under light-limited conditions,
283 whereas it might enhance photoinhibition at light levels above saturation (Gao et al., 2012b).
284 In high-CO_2-grown cells of the diatom *Phaeodactylum tricornutum*, the electron transport rate
285 from photosystem II (PSII) was photoinhibited to a greater extent than in low-CO_2-grown
286 cells under light stress (Wu et al., 2010). The combination of exposure to increased light and
287 CO_2 levels reduced photosynthetic carbon fixation of phytoplankton in the South China Sea
288 (Gao et al., 2012b). These observations are consistent with the CCM serving as a sink for
289 excessive energy (Wu et al., 2010), so its downregulation causes stimulation of high light
290 stress. In our findings, however, elevated CO_{2aq} (LpH) imposed negative effects on *P. globosa*
291 grown at either low (growth limiting) or high (saturating) light levels (Fig. 3), which might be
292 associated with the intrinsic properties of the alga. A constitutive CCM, the activity of which
293 was not affected by increases in CO_{2aq}, has been found in *P. globosa* (Rost et al., 2003; Chen
294 and Gao, 2011). Therefore, the responses of *P. globosa*'s growth or photosynthesis to the
295 acidification cannot be linked to energy costs associated with downregulation of CCMs. The
296 contrasting responses of the diatom *Phaeodactylum tricornutum* (Wu et al., 2010; Gao et al.,
297 2012b) and *P. globosa* (present work) to ocean acidification reflect highly different strategies
298 that different taxa employ to cope with the changes in carbonate chemistry of seawater.
299 While *Phaeocystis globosa* cells became acclimated to the acidification, they synthesised
300 more pigments (Fig. 2) and performed better photochemistry (increased yield and decreased

photoinhibitory non-photochemical quenching) (Fig. 1, 3 and Table 2), suggesting that the alga possesses the potential to cope with the chemical changes induced by elevated CO_2 (lowed pH). The rate of acclimation to LpH, however, appeared to depend on irradiance levels. At day 1 (1 generation), the cells grown at the LpH (high-CO_2) either under middle or high light levels all showed reduced growth rate and quantum yield (Fig. 1, 3), whereas by day 7 (19 generations) their growth and yield became enhanced under the middle and high light levels (Fig. 1, 3), compared to those grown at HpH. Increased acidity in the ambient seawater might, to some extent, affect intracellular acid-base balance, and hence cause a decrease in effective photochemical efficiency and an increase in NPQ (Fig. 3). During the acclimation, the state transition quenching (qT) of fluorescence increased significantly (Table 2), suggesting that the ratio of PSI to PSII activity in the algal cells increases, driving more cyclic electron transport to produce additional ATP, which may alleviate the stresses caused by high light to the PSII reaction center as well as the acidification of the stroma. While the energy-dependent quenching (qE), photoinhibition quenching (qI) (Table 2) and light requirement for saturating photosynthetic rate (I_k, Table 3) all increased in the cells exposed to LpH at day 1, these parameters declined, after 7 days acclimation to the LpH, to be comparable to those in the HpH-grown cells. During the acclimation, qI decreased with increases in cellular photosynthetic pigments (Fig. 2, Table 2), supporting the notion that increase in tolerance of the acidification stress was associated with increased light capture and use efficiency (Fig. 2, Tables 2,3). The time span for such acclimation was longer under high light than in low light, reflecting that growth-stressful light levels delay the acclimation, probably due to additional energy costs for the cells to cope with photoinhibition.

The apparent effects of CO_2-induced acidification on *P. globosa* depend on the balance between the positive effects of increased CO_{2aq} availability per se and the negative impacts of simultaneous acidification. The former increases with increases in CO_{2aq}, whereas the latter

stress (OA) is enhanced with increasing acidification (Fig. 4). Hypothetically, when the positive effect (CO_2) is balanced by the negative impact (pH and chemical changes), algal photosynthesis shows an inflexion point, a tipping point, beyond which net photosynthesis decreased progressively (Fig. 4). Elevated pCO_2 could enhance algal photosynthesis by improving CO_2 supply to the active site of the carboxylating enzyme Rubisco (Raven et al., 2003, 2008) or by indirect energy supply from downregulated CCMs (Gao et al., 2012a). The acidification, however, together with other chemical changes, could alter periplasmic redox activity or the permeability of cellular membranes (Sobrino et al., 2005) and perturb ion channels across the cell membrane, therefore acting as a stressor and increasing mitochondrial respiration (Wu et al., 2010; Yang and Gao, 2012). The inflexion point from positive to negative effects of elevated CO_2 was affected by increases in light intensity and the degree of acclimation to acidification (Fig. 4). The tipping point was higher in cells grown under LL or LpH, compared to those grown under HL or HpH (Fig. 4).

Algal responses to OA can be species-specific (even strain-specific) (Langer et al., 2006, 2009; Beardall et al., 2009; Trimborn et al., 2013) and depend on multiple climate change factors (Gao *et al*., 2012b). The ecological effects of CO_2-induced acidification on *P. globosa* will probably be dependent on its ecological niche or ecosystem. In coastal waters, diel pH changes with day-night pH oscillations can expose the cells to fast pH and carbonate chemistry changes, additional OA forcing in such ecosystem may lead to different responses of the alga to climate change. *P. globosa* is prone to take advantage under high pH (or low CO_{2aq}) conditions due to its highly efficient CCM, compared to algae with less active CCMs (Berry et al., 2002). While the pH value decreases rapidly in waters due to either heavy rainfall, or seasonal upwelling, or eutrophication and deoxygenation (Cai et al., 2011), *P. globosa* may experience disadvantageous situations, with increases in CO_2 in the atmosphere and increased irradiance due to enhanced stratification (Boyd and Doney 2002). This may

cause a shift in algal community structure at different latitudes and seasons with increasing pCO_2 in the atmosphere. However, our data do suggest that *P. globosa* has the capability to acclimate to the expected rise in atmospheric CO_2 to 1000 ppmv by the end of the century, so the ways in which it will be influenced ecologically, as part of the broad algal community, in the long term remain to be seen.

In conclusion, the red tide alga, *P. globosa*, can increase its tolerance to lowered pH after it had acclimated to the CO_2-induced seawater acidification. Mechanistically, the alga increased its photosynthetic and photoprotective pigments and raised its energy use efficiency and excessive energy dissipation strategy. Along with its constitutive CCM and associated energetics, *P. globosa* can increase its competitiveness in phytoplankton communities under OA and simultaneously increased irradiance due to enhanced stratification.

Acknowledgements

This study was supported by Joint project of NSFC and Shandong province (Grant No. U1406403), National Natural Science Foundation (No. 40930846, No. 41120164007), Strategic Priority Research Program of CAS (Grant No. XDA11020302), National Basic Research Program of China (2011CB200902), Program for Changjiang Scholars and Innovative Research Team (IRT0941) and China-Japan collaboration project from MOST (S2012GR0290). JB's work on climate change effects on algae has been funded by the Australian Research Council and his visit to Xiamen was supported by "111" project from Minstry of Education.

References

Arnold, H. E., Kerrison, P., and Steinke, M.: Interacting effects of ocean acidification and warming on growth and DMS production in the haptophyte coccolithophore *Emiliania huxleyi*. Global Chang. Biol., 19, 1007-1016, doi:10.1111/gcb.12105, 2013.

Barry, J. P., Tyrrell, T., Hansson, L., Plattner, G., and Gattuso, J.: Atmospheric CO_2 targets for ocean acidification pertubation experiments. In: Guide to Best Practices in Ocean Acidification Research and Data Reporting, edited by: Riebesell, U., Fabry, V. J., Hansson, L., and Gattuso, J., Luxembourg Press, Belgium, 53–64, 2010.

Beardall, J., Sobrino, C., and Stojkovic, S.: Interactions between the impacts of ultraviolet radiation, elevated CO_2, and nutrient limitation on marine primary producers. Photochem. Photobiol. Sci., **8**, 1257-1265, doi:10.1039/B9PP00034H, 2009.

Berry, L., Taylor, A. R., Lucken, U., Ryan, K. P., and Brownlee, C.: Calcification and inorganic carbon acquisition in coccolithophores. Funct. Plant Biol., **29**, 289–299, doi:10.1071/PP01218, 2002.

Bilger, W. and Björkman, O.: Role of the xanthophylls cycle in photoprotection elucidated by measurements of light-induced absorbance changes, fluorescence and photosynthesis in leaves of *Hedera canariensis*. Photosyn. Res., **25**, 173–185, doi:10.1007/BF00033159, 1990.

Boyd, P. W. and Doney, S. C.: Modeling regional responses by marine pelagic ecosystems to global climate change. Geophys. Res. Lett., **29**, 53-1– 53-4, doi:10.1029/2001GL014130, 2002.

Brussaard, C. P. D., Noordeloos, A. A. M., Witte, H., Collenteur, M. C. J., Schulz, K., Ludwig, A., and Riebesell, U.: Arctic microbial community dynamics influenced by elevated CO 2 levels. Biogeosciences, 10(2), 719-731, doi:10.5194/bg-10-719-2013, 2013.

Cai, W. J., Hu, X., Huang, W. J., Murrell, M. C., Lehrter, J. C., Lohrenz, S. E., Chou, W ,

Zhai, W., Hollibaugh, J. T., Wang, Y., Pingsan Zhao, P., Xianghui Guo, X., Gundersen, K., Dai, M., and Gong, G. C.: Acidification of subsurface coastal waters enhanced by eutrophication. Nat. Geosci., **4**, 766-770, doi:10.1038/ngeo1297, 2011.

Chen, S. and Gao, K.: Solar ultraviolet radiation and CO_2-induced ocean acidification interacts to influence the photosynthetic performance of the red tide alga *Phaeocystis globosa* (Prymnesiophyceae). Hydrobiologia, **1**, 105-117, doi:10.1007/s10750-011-0807-0, 2011.

Chen, Y. Q., Wang, N., Zhang, P., Zhou, H., and Qu, L. H.: Molecular evidence identifies bloom-forming *Phaeocystis* (Prymnesiophyta) from coastal waters of southeast China as *Phaeocystis globosa*. Biochem. System. Ecol., **30**, 15– 22, doi:org/10.1016/S0305-1978(01)00054-0, 2002.

Cornwall, C. E., Hepburn, C. D., McGraw, C. M., Currie, K. I., Pilditch, C. A., Hunter, K. A., and Hurd, C. L.: Diurnal fluctuations in seawater pH influence the response of a calcifying macroalga to ocean acidification. Pro. Roy. Soc. B: Biol. Sci., **280**, 1772-1780, 2013.

Gao, K., Aruga, Y., Ishihara, T., Akano, T., and Kiyohara, M.: Enhanced growth of the red alga *Porphyra yezoensis* Ueda in high CO_2 concentrations. J. Appl. Phycol., **3**, 355–362, doi:10.1007/BF00026098, 1991.

Gao, K., Guan, W., and Helbling, E. W.: Effects of solar ultraviolet radiation on photosynthesis of the marine red tide alga *Heterosigma akashiwo* (Raphidophyceae). J. Photochem. Photobiol. B, **86**, 936–951, doi:org/10.1016/j.jphotobiol.2006.05.007, 2007.

Gao, K. and Zheng, Y.: Combined effects of ocean acidification and solar UV radiation on photosynthesis, growth, pigmentation and calcification of the coralline alga *Corallina sessilis*. Global Chang. Biol., **16**, 2388–2398, doi:10.1111/j.1365-2486.2009.02113.x, 2010.

Gao, K., Helbling, E. W., Häder, D. P., and Hutchins, D. A.: Responses of marine primary producers to interactions between ocean acidification, solar radiation, and warming. Mar.

Ecol. Prog. Ser., **470**, 167-189, doi:10.3354/meps10043, 2012a.

Gao, K., Xu, J., Gao, G., Li, Y., Hutchins, D. A., Huang, B., Wang, L., Zheng, Y., Peng Jin, P., Cai, X., Häder, D-P., Li, W., Xu, K., Liu, N., and Riebesell, U.: Rising CO_2 and increased light exposure synergistically reduce marine primary productivity. Nat. Clim. Chang. **2**, 519–523, doi:10.1038/nclimate1507, 2012b.

Gao, K. and Campbell, D. A.: Photophysiological responses of marine diatoms to elevated CO2 and decreased pH: a review. Funct. Plant Biol. **41**, 449-459, doi.org/10.1071/FP13247, 2014.

Genty, B., Briantais, J. M., and Baker, N. R.: The relationship between the quantum yield of photosynthetic electron transport and quenching of chlorophyll fluorescence. Biochim. Biophys. Acta, **990**, 87–92, doi:org/10.1016/S0304-4165(89)80016-9, 1989.

Hein, M. and Sand-Jensen, K.: CO_2 increases oceanic primary production. Nature, **388**, 526–27, 1997.

Hoogstraten, A., Peters, M., Timmermans, K. R., and Baar, H. D.: Combined effects of inorganic carbon and light on *Phaeocystis globosa* Scherffel (Prymnesiophyceae). Biogeosciences, **9**, 1885–1896, doi:10.5194/bg-9-1885-2012, 2012.

IPCC: Summary for policymakers. In: Climate Change 2007: The Physical Science Basis Contribution of Working Group I to the Fourth Assessment Report of the IPCC, edited by: Solomon, S., Qin, D., Manning, M., et al., CambridgeUniversity Press, Cambridge, 996pp, 2007.

Jeffrey, S. W. and Welschmeyer, N. A.: Spectrophotometric and fluorometric equations in common use in oceanography. In: Phytoplankton pigments in oceanography: guidelines to modern methods, edited by: Jeffrey, S. W., Mantoura, R. F. C., and Wright, S. W., UNESCO Publish, Paris, 597–621, 1997.

Langer, G., Geisen, M., Baumann, K. H., Kläs, J., Riebesell, U., Thoms, S., and Young, J. R.:

476 Species-specific responses of calcifying algae to changing seawater carbonate chemistry.
477 Geochem. Geophys. Geosys., **7**, Q09006, doi:10.1029/2005GC001227, 2006.
478 Langer, G., Nehrke, G., Probert, I., Ly, J., & Ziveri, P.: Strain-specific responses of *Emiliania*
479 *huxleyi* to changing seawater carbonate chemistry. Biogeosciences, **6**, 2637–2646,
480 doi:10.5194/bg-9-1885-2012, 2009.
481 LaRoche J, Rost B, and Engel A: Bioassays, batch culture and chemostat experimentation. In:
482 Guide to Best Practices in Ocean Acidification Research and Data Reporting, edited by:
483 Riebesell, U., Fabry, V. J., Hansson, L., and Gattuso, J., Luxembourg Press, Belgium, 81-94,
484 2010.
485 Lewis, E. and Wallace, D. W. R.: Program developed for CO_2 system calculations [Internet].
486 Carbon Dioxide Information Analysis Center, Oak Ridge National Laboratory US,
487 Department of Energy. Available from
488 http://cdiac.ornl.gov/ftp/co2sys/CO2SYS_calc_DOS_v1.05/. Accessed 21-Dec-2012.
489 Lichtenthaler, H. K., Buschmann, C., and Knapp, M.: How to correctly determine the
490 different chlorophyll fluorescence parameters and the chlorophyll fluorescence decrease
491 ratio R_{Fd} of leaves with the PAM fluorometer. Photosynthetica, **43**, 379-393,
492 doi:10.1007/s11099-005-0062-6, 2005.
493 Peperzak, L. and Poelman, M.: Mass mussel mortality in the Netherlands after a bloom of
494 *Phaeocystis globosa* (Prymnesiophyceae). J. Sea Res., 60, 220–222,
495 doi:org/10.1016/j.seares.2008.06.001, 2008.
496 Peperzak, L. and Gäbler-Schwarz, S.: Current knowledge of the life cycles of *Phaeocystis*
497 *globosa* and *Phaeocystis antarctica* (Prymnesiophyceae). J. Phycol., **48**, 514-517,
498 doi:org/10.1016/0924-7963(94)90014-0, 2012.
499 Platt, T., Gallegos, C. L., and Harrison, W. G.: Photoinhibition of photosynthesis in natural
500 assemblages of marine phytoplankton. J. Mar. Res., **38**, 687-701, 1980.

Ralph, P. J.: Rapid light curves: A powerful tool to assess photosynthetic activity. Aquat. Bot., **82**, 222-237, doi:org/10.1016/j.aquabot.2005.02.006, 2005.

Raven, J. A. and Geider, R. J.: Adaptation, and regulation in algal photosynthesis. In: Photosynthesis in algae, edited by: Larkum, A. W. D., Douglas, S., and Raven, J. A., Kluwer Academic Publishers, Netherlands, 385-412, 2003.

Raven, J. A., Cockell, C. S., and Rocha, C. L. D.: The evolution of inorganic carbon concentrating mechanisms in photosynthesis. Phil. Trans. Roy. Soc. B, **363**, 2641-2650, doi:10.1098/rstb.2008.0020, 2008.

Raven, J. A.: Effects on marine algae of changed seawater chemistry with increasing atmospheric CO_2. Biology and Environment: Pro. Roy. Ir. Acad., **111**, 1-17, doi:10.1098/rstb.2008.0020, 2011.

Riebesell, U., Zondervan, I., Rost, B., Tortell, P. D., Zeebe, R. E., and Morel, F. M.: Reduced calcification of marine plankton in response to increased atmospheric CO_2. Nature, **407**, 364–366, doi:10.1038/35030078, 2000.

Ritchie, R. J.: Consistent sets of spectrophotometric chlorophyll equations for acetone, methanol and ethanol solvents. Photosyn. Res., **89**, 27–41, doi:10.1007/s11120-006-9065-9, 2006.

Rosner, B. A.: Fundamentals of biostatistics. **7**th edition, Duxbury Press, New York, 516pp, 2011.

Rost, B., Riebesell, U., Burkhardt, S., & Sültemeyer, D.: Carbon acquisition of bloom-forming marine phytoplankton. Limnol. Oceanogr., **48**, 55–67, 2003.

Rousseau, V., Chrétiennot-Dinet, M. J., Jacobsen, A., Verity, P., and Whipple, S.: The life cycle of *Phaeocystis*: state of knowledge and presumptive role in ecology. Biogeochemistry, **83**, 29-47, doi:10.1007/s10533-007-9085-3, 2007.

Schoemann, V., Becquevort, S., Stefels, J., Rousseau, V., and Lancelot, C.: *Phaeocystis*

526 blooms in the global ocean and their controlling mechanisms: a review. J. Sea Res., **53**,
527 43-66, doi:org/10.1016/j.seares.2004.01.008, 2005.
528 Sobrino, C., Neale, P. J., and Lubian, L. M.: Interaction of UV radiation and inorganic carbon
529 supply in the inhibition of photosynthesis: Spectral and temporal response of two marine
530 picoplankton. J. Photochem. Photobiol. B, **81**, 384–393,
531 doi:10.1111/j.1751-1097.2005.tb00198.x, 2005.
532 Tanaka, T., Alliouane, S., Bellerby, R. G. B., Czerny, J., Kluijver, A. D., Riebesell, U., Schulz,
533 K. G., Silyakova, A., and Gattuso, J. P.: Effect of increased pCO 2 on the planktonic
534 metabolic balance during a mesocosm experiment in an Arctic fjord. Biogeosciences, 10(1),
535 315-325, doi:10.5194/bg-10-315-2013, 2013.
536 Trimborn, S., Brenneis, T., Sweet, E., and Rost, B.: Sensitivity of Antarctic phytoplankton
537 species to ocean acidification: Growth, carbon acquisition, and species interaction. Limnol.
538 Oceanogr., **58**, 997-1007, doi:10.4319/lo.2013.58.3.0997, 2013.
539 Wang, Y., Smith, J., and Wang, X., Li, S.: Subtle biological responses to increased CO_2
540 concentrations by *Phaeocystis globosa* Scherffel, a harmful algal bloom species. Geophys.
541 Res. Lett., **37**, L09604, doi:10.1029/2010gl042666, 2010.
542 Wu, H., Zou, D., and Gao, K.: Impacts of increased atmospheric CO_2 concentration on
543 photosynthesis and growth of micro- and macro-algae. Sci. China Ser. C: Life Sci., **51**,
544 1144-1150, doi:10.1007/s11427-008-0142-5, 2008.
545 Wu, Y., Gao, K., and Riebesell, U.: CO_2-induced seawater acidification affects physiological
546 performance of the marine diatom *Phaeodactylum tricornutum*. Biogeosciences, **7**,
547 2915–2923, doi:10.5194/bgd-7-3855-2010, 2010.
548 Yang, G. and Gao, K.: Physiological responses of the marine diatom *Thalassiosira*
549 *pseudonana* to increased pCO_2 and seawater acidity. Mar. Environ. Res., **79**, 142-151,
550 doi:org/10.1016/j.marenvres.2012.06.002, 2012.

Zou, D., Gao, K., and Luo, H.: Short- and long- term effects of elevated CO_2 on photosynthesis and respiration in the marine macroalga *Hizikia fusiformis* (Sargrassaceae, Phaeophyta) grown at low and high N supplies. J. Phycol., **47**, 87–97, doi:10.1111/j.1529-8817.2010.00929.x, 2011.

Table 1 Parameters of the seawater carbonate system under ambient (39.3 Pa or 390 μatm) and enriched (101.3 Pa or 1000 μatm) CO_2 levels in the turbidostat cultures under different photon flux densities (LL: 25, ML: 200, HL: 800 μmol photons m^{-2} s^{-1}) of PAR. Dissolved inorganic carbon (DIC), pH, salinity (33 ‰), nutrient concentration (phosphate, 3.6; silicate, 11.3; nitrate, 882.4 μM), and temperature (20 ^{o}C) were used to derive all other parameters using the CO_2 system analyzing software CO2SYS. The stoichiometric equilibrium constants K_1 and K_2 for carbonic acid used were 6.04 and 9.16, respectively. The data represents the mean ± SD (n=24) except TA_m (n = 9). Superscripts with different letters indicate significant differences between groups.

	39.3 Pa CO_2			101.3 Pa CO_2		
	LL	ML	HL	LL	ML	HL
pH	8.08 ± 0.02 ^{a}	8.09 ± 0.02 ^{a}	8.09 ± 0.03 ^{a}	7.70 ± 0.03 ^{b}	7.71 ± 0.02 ^{b}	7.70 ± 0.03 ^{b}
DIC (μM)	2011.3 ± 97.2 ^{c}	2006.6 ± 106.1 ^{c}	2007.8 ± 103.5 ^{c}	2213.6 ± 100.4^{d}	2187.2 ± 104.8 ^{d}	2168.3± 91.8 ^{d}
HCO_3^- (μM)	1797.1 ± 83.4 ^{e}	1789.0 ± 77.3 ^{e}	1790.1 ± 90.4 ^{e}	2082.3 ± 93.6 ^{f}	2056.1± 101.3 ^{f}	2039.7 ± 96.6 ^{f}
CO_2aq (μM)	12.1 ± 0.5 ^{g}	11.8 ± 0.5 ^{g}	11.8 ± 0.6 ^{g}	33.7 ± 0.8 ^{h}	32.5 ± 0.7 ^{h}	33.0 ± 0.9 ^{h}
CO_3^{2-} (μM)	202.0 ± 7.5 ^{p}	205.8 ± 6.6 ^{p}	205.9 ± 6.8 ^{p}	97.6 ± 3.9 ^{q}	98.6 ± 3.7 ^{q}	95.6 ± 3.2. ^{q}
TA (μM)	2287.6 ± 97.1^{n}	2288.7 ± 103.2^{n}	2290.0 ± 95.3^{n}	2318.6 ± 99.7^{n}	2295.3 ± 96.4^{n}	2272.0± 103.1^{n}
TA_m(μM)	2271.3 ± 101.6^{n}	2268.2 ± 107.1^{n}	2272.6 ± 102.6^{n}	2288.6 ± 113.8^{n}	2269.6 ± 97.8^{n}	2243.6 ± 109.3^{n}

584

585 **Table 2** The energy-dependent (qE), state-transition (qT) and photoinhibition quenching (qI) of *P. globosa* at generation 1 and generation 19 ,

586 grown in pH 7.70 culture under different irradiance levels (LL, 25; ML, 200; HL, 800 μmol photons·m^{-2}·s^{-1}), respectively. Superscripts with

587 different letters indicate significant differences between groups. The data represent the mean ± SD (n=3, triplicate cultures).

	qE		qT		qI	
Generation 1	LpH/HC	HpH/LC	LpH/HC	HpH/LC	LpH/HC	HpH/LC
LL	0.09 ± 0.01^{a}	0.07 ± 0.01^{c}	0.15 ± 0.01^{g}	0.11 ± 0.02^{h}	0.14 ± 0.02^{q}	0.08 ± 0.01^{p}
ML	0.16 ± 0.03^{bdef}	0.12 ± 0.02^{bd}	0.16 ± 0.02^{mgk}	0.13 ± 0.02^{hg}	0.31 ± 0.03^{s}	0.16 ± 0.03^{vq}
HL	0.21 ± 0.03^{bef}	0.15 ± 0.02^{bdef}	0.18 ± 0.02^{k}	0.15 ± 0.02^{g}	0.51 ± 0.05^{t}	0.23 ± 0.03^{r}
Generation 19						
LL	0.16 ± 0.01^{bde}	0.07 ± 0.01^{c}	0.17 ± 0.02^{gk}	0.11 ± 0.02^{h}	0.12 ± 0.01^{zq}	0.09 ± 0.02^{p}
ML	0.21 ± 0.02^{bef}	0.13 ± 0.02^{bd}	0.19 ± 0.03^{mk}	0.14 ± 0.01^{hg}	0.18 ± 0.02^{vq}	0.15 ± 0.02^{q}
HL	0.24 ± 0.02^{bf}	0.16 ± 0.01^{bde}	0.23 ± 0.04^{m}	0.15 ± 0.02^{g}	0.24 ± 0.03^{r}	0.22 ± 0.03^{r}

588

589

590

591

Table 3 The photosynthetic light-harvesting efficiency (α), maximum photosynthetic rate (P_m) and light saturation point (I_k), derived from light-response curves for *P. globosa* cells incubated in either pH 8.07 or pH 7.70 (induced by high CO_2) cultures. The cells were grown in pH 8.07 culture for about 9 generations, and in pH 7.70 (induced by high CO_2) culture for 1 generation (G_1) or 19 generations (G_{19}), , under an irradiance of 200 μmol photons·m^{-2}·s^{-1} before the light-response curve was measured. Superscripts with different letters indicate significant differences between groups. The data represent the mean ± SD (n=3, triplicate cultures)**.**

	α	P_m (μmol O_2·(μg Chl)$^{-1}$·h^{-1})	I_k (μmol photons·m^{-2}·s^{-1})
pH 8.07	0.007±0.001^a	0.360±0.014^c	51.4±3.66^g
pH 7.70 (G_1)	0.003±0.001^b	0.318±0.019^d	106.0±4.39^h
pH 7.70 (G_{19})	0.006±0.001^a	0.354±0.015^c	59.0±5.41^g

612

613 ***Figure captions***

614 **Fig. 1** The specific growth rates (open symbols) of *P. globosa* grown at pH 8.07 and the ratios
615 (solid symbols) of the specific growth rate at pH 7.70 to that at pH 8.07 ($\mu_{7.70}$: $\mu_{8.07}$) under
616 different irradiance levels (LL, 25; ML, 200; HL, 800 μmol photons·m^{-2}·s^{-1}), respectively. The
617 data represent the mean ± SD (n=3, triplicate cultures).

618 **Fig. 2** Contents of chlorophyll (a) and carotenoids (b) of *P. globosa* cells grown at pH 8.07
619 (open symbols) and the ratios (solid symbols) of the pigments at pH 7.70 to that at pH 8.07
620 under different irradiance levels (LL, 25; ML, 200; HL, 800 μmol photons·m^{-2}·s^{-1}),
621 respectively. The data represent the means ± SD (n=3, triplicate cultures)**.**

622 **Fig. 3** Effective quantum yield (Yield) (a) and non-photochemical quenching (NPQ) (b) of *P.*
623 *globosa* grown at pH 8.07 (open symbols), and the ratios (solid symbols) of either the yield or
624 the NPQ at pH 7.70 to that at pH 8.07 under different irradiance levels (LL, 25; ML, 200; HL,
625 800 μmol photons·m^{-2}·s^{-1}), respectively. The data represent the means ± SD (n=3, triplicate
626 cultures)**.**

627 **Fig. 4** Net photosynthesis of *P. globosa* cells, acclimated to either pH8.07 or pH7.70 cultures
628 in the corresponding irradiances to the measurement for 3 days (9 generations), under
629 irradiances of (a) 25 and (b) 200 μmol photon s·m^{-2}·s^{-1} at different pH levels induced by
630 different CO_{2aq} concentrations. The data represent the means ± SD in triplicate incubations. *
631 and ** indicate significant differences between the two pH levels at $p<0.05$ and $p<0.01$,
632 respectively.

633

634

635

636

Fig. 1

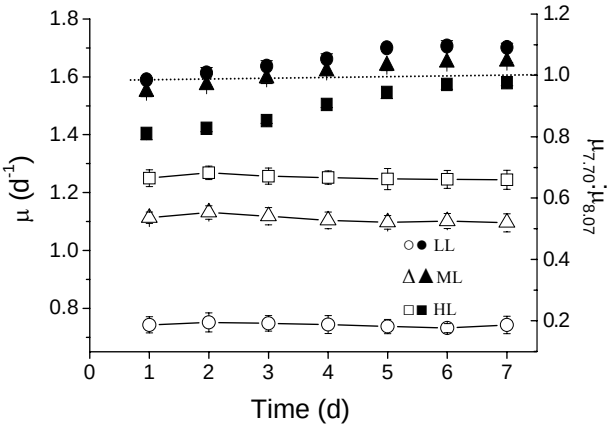
1.8
1.6
1.4
1.2
1.0
0.8
μ (d-1)
1.2
1.0
0.8
0.6
0.4
0.2
μ7.70:μ8.07
LL
ML
HL
0
1
2
3
4
5
6
7
Time (d)

Fig. 2

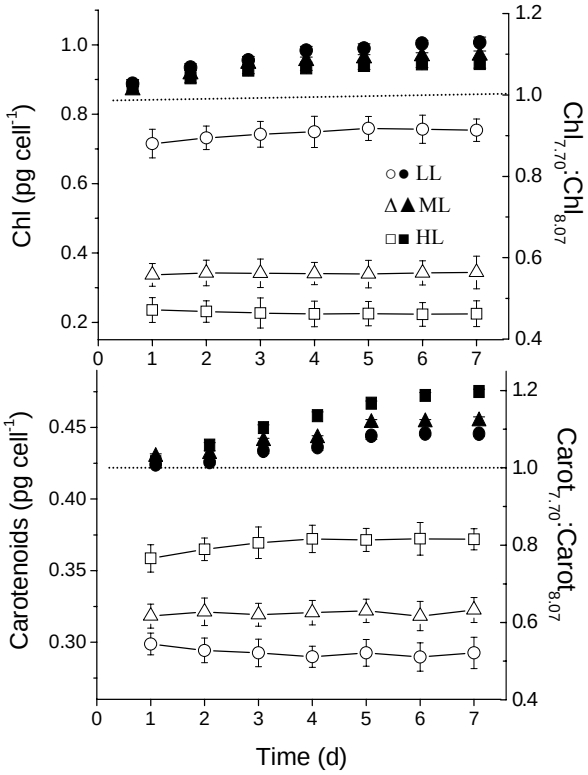
Chl (pg cell^{-1})
Chl$_{7.70}$:Chl$_{8.07}$
LL
ML
HL
Carotenoids (pg cell^{-1})
Carot$_{7.70}$:Carot$_{8.07}$
Time (d)

Fig. 3

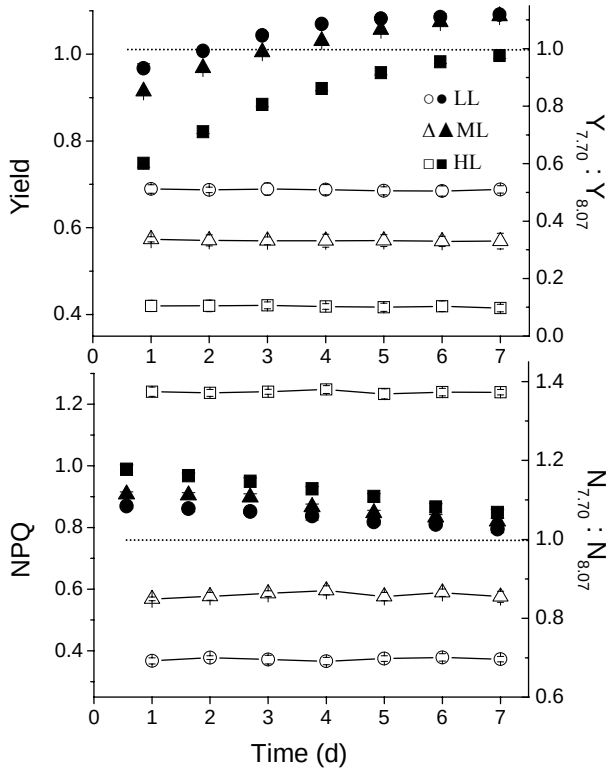

Fig. 4

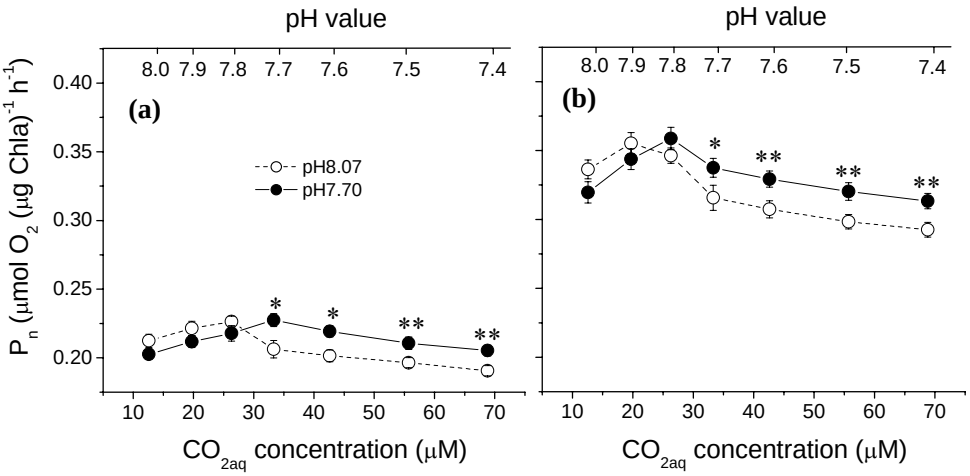
pH value
8.0 7.9 7.8 7.7 7.6 7.5 7.4
(a)
(b)
pH8.07
pH7.70
P_n (μmol O_2 (μg Chla)$^{-1}$ h^{-1})
0.40
0.35
0.30
0.25
0.20
*
**
10 20 30 40 50 60 70
CO_{2aq} concentration (μM)